

Capacity and Energy Trade-Offs in FR3 6G Networks Using Real Deployment Data

David López-Pérez[‡], Nicola Piovesan[§], and Matteo Bernabè[‡]

[‡]Universitat Politècnica de València, Spain [§]Huawei Technologies, France

Abstract—This article presents a data-driven system-level analysis of multi-layer 6G networks operating in the upper mid-band (FR3: 7–24 GHz). Unlike most prior studies based on 3rd Generation Partnership Project (3GPP) templates, we leverage real-world deployment and traffic data from a commercial 4G/5G network in China to evaluate practical 6G strategies. Using *Giulia*—a deployment-informed system-level heterogeneous network model—we show that 6G can boost median throughput by up to 9.5× over heterogeneous 4G+5G deployments, but also increases power usage by up to 59 %. Critically, co-locating 6G with existing sites delivers limited gains while incurring high energy cost. In contrast, non-co-located, traffic-aware deployments achieve superior throughput-to-watt efficiency, highlighting the need for strategic, user equipment (UE) hotspot-focused 6G planning.

I. INTRODUCTION

In contrast to the ambitious roadmaps often envisioned for the sixth generation (6G) of the mobile network technology, we argue that its commercial realization will likely center on a narrower set of practical features. Much like fifth generation (5G) deployments, which ultimately realized a few high-impact technologies—most notably massive multiple-input multiple-output (mMIMO), ultra-reliable low latency communication (URLLC), and network slicing [1]—, we expect 6G to follow a similarly selective trajectory. This pragmatic focus is especially relevant in the current macroeconomic climate, where rising infrastructure costs and uncertain revenue models are reshaping investment strategies across the telecommunications sector.

Among the features likely to define early 6G rollouts, we identify three foundational enablers that are likely to be both technically mature and economically viable by 2030 [2]:

- *Extreme mMIMO at centimeter (cm)-wave (7–24 GHz)*: A cornerstone for scalable, high-capacity deployments, cm-wave extreme mMIMO will combine wide bandwidth availability with favorable propagation and implementation characteristics, making it ideal for next-generation urban and indoor networks.
- *Artificial intelligence (AI)*: Deeply embedded across the protocol stack, AI will allow the smart and dynamic orchestration of heterogeneous 4G/5G/6G networks, supporting functions such as load balancing, interference mitigation, and energy-efficient scheduling.
- *Sensing*: By equipping networks with environmental awareness, sensing technologies will enable new services

such as autonomous driving and smart infrastructure. Additionally, sensing data will enhance AI-driven network intelligence through real-time contextual feedback.

Among these, cm-wave extreme mMIMO stands out as the anchor technology for delivering the multi-gigabit-per-second capacity demanded by emerging 6G use cases. It can achieve this capacity, while circumventing many of the deployment challenges inherent to millimeter (mm)-wave systems, including high energy usage, blockage sensitivity, as well as poor indoor penetration and challenging mobility management [3].

A. Network Optimization Challenge

Designing and optimizing the resulting complex, heterogeneous 4G/5G/6G networks, especially in dense urban environments, will increasingly exceed the limits of current human-based engineering. This growing complexity calls for a shift toward AI-driven orchestration and adaptation. However, the effectiveness of these AI-based strategies critically depends on the availability of accurate, realistic models for training and evaluation.

Yet much of the current cellular modeling landscape remains rooted in 3rd Generation Partnership Project (3GPP)-style deployment templates and abstract traffic assumptions [4], which fail to capture the local spatial, temporal, and topological complexities of real-world networks. This gap can lead to misleading assessments of system performance, especially in multi-layer deployments that integrate legacy and next-generation technologies.

What is needed instead is a data-driven, deployment-informed modeling framework—one that reflects actual site layouts, hardware configurations, user behaviors, and traffic patterns. Such models are essential for evaluating true system-level trade-offs in coverage, throughput, latency, and energy usage under realistic operational conditions.

B. Contributions of This Work

In this article, we present a comprehensive, data-driven system model for—and analysis of—multi-layer 6G deployments operating in the upper mid-band spectrum, building upon and significantly advancing our earlier work [2]. This study departs from synthetic assumptions and embraces realism through direct integration of live network data, enabling a much more accurate exploration of next-generation architectures.

At the heart of our analysis lies *Giulia*—a high-fidelity, system-level simulator purpose-built for evaluating heterogeneous cellular networks. Unlike conventional tools that

rely primarily on abstracted or idealized models, *Giulia* is designed to integrate real-world engineering data and AI models whenever available. In scenarios where such data is not accessible, it remains compatible with standard 3GPP assumptions, ensuring analytical continuity. The digital twin captures detailed aspects of base station (BS) and user equipment (UE), network configuration, radio propagation, mMIMO, scheduling behavior, beamforming strategies, and power consumption with deployment-grade precision. Importantly, and unlike most tools, *Giulia* supports per-cell radio customization—each cell can be powered by radios with distinct characteristics and configurations.

Key contributions of this article include:

- *Deployment-Informed Network Modeling*: Leveraging proprietary datasets from a commercial urban network in China, we extract true-to-life spatial layouts, engineering parameters, and load distributions across 4G, 5G, and synthetic 6G layers.
- *Realistic System-Level Simulation*: Using *Giulia*, we simulate end-to-end system behavior with fidelity using a mix of expert-, 3GPP-, and AI-based models, offering a holistic view of capacity and energy trade-offs.
- *Comparative Evaluation of Deployment Strategies*: We examine multiple architectural variants—including co-located, non-co-located, and traffic-driven hotspot deployments of 6G cm-wave cells—and benchmark them against legacy 4G/5G baselines to uncover insights into spectrum utilization, energy efficiency, and spatial densification.

The remainder of this article is organized as follows. Section II reviews recent advances in cm-wave extreme mMIMO. Section III introduces *Giulia*, our data-driven system model. Section IV presents our performance evaluation of heterogeneous 4G/5G/6G networks, highlighting trade-offs across different deployment strategies. Finally, Section V concludes the article with a summary of findings and future research directions.

II. FR3 CM-WAVE EXTREME MIMO

The upper mid-band spectrum from 7 to 24 GHz, referred to by 3GPP as frequency range 3 (FR3) [5], is a strong candidate for early 6G deployments. FR3 sits between sub-6 GHz spectrum (FR1), which offers wide-area coverage but limited bandwidth, and mm-wave bands FR2, which offer very large bandwidth but suffer from severe propagation losses. This intermediate position makes FR3 attractive for dense urban networks that need multi-gigabit capacity without the fragility typically associated with FR2.

To translate FR3 bandwidth into cell-level capacity, BSs must also deliver substantially higher beamforming and spatial-multiplexing gains than today's sub-6 GHz systems. This requires antenna-array and radio designs that scale to very large active panels while keeping cost and power consumption manageable. This trend is driving *extreme* mMIMO, with thousands of antenna elements and well over 128 TRX chains, enabling narrow beams and high-order spatial multiplexing [6],

[7]. When paired with UE devices equipped with up to 64 antennas, FR3-based extreme mMIMO may support up to 20 spatial streams per device, enabling peak data rates approaching 50 Gbps [7].

A. Opportunities and Performance Advantages

Compared to FR2 deployments:

- FR3 provides channel bandwidths comparable to FR2 (up to 400 MHz) while offering more robust coverage in dense urban layouts, enabling broader service areas and more reliable non line of sight (NLoS) connectivity.
- For outdoor-to-indoor users in particular, the longer wavelength reduces penetration loss and sensitivity to shadowing, improving cell-edge stability and indoor service continuity [8].
- Beam training is less complex due to wider beams and slower beam/angle variation under mobility, reducing control overhead.
- Lower carrier frequencies improve hardware efficiency, with less stringent phase-noise and power-amplifier requirements [5].

FR3 thus delivers much of the spectral capacity of FR2 while avoiding critical deployment drawbacks such as poor mobility management, bad indoor penetration, blockage sensitivity, and excessive power demand [3].

B. Deployment Challenges at FR3

While FR3 presents a compelling balance between capacity and coverage, its practical realization demands navigating a range of physical, architectural, and regulatory hurdles. Chief among these are channel propagation losses and the scaling of energy usage-issues that, although less severe than in FR2 (mm-Wave), remain significant bottlenecks. These challenges cluster into five primary domains:

1) *Propagation and Coverage Trade-offs*: The key propagation challenge of FR3 lies in its frequency-dependent path loss. Empirical measurements indicate that moving from 3.5 GHz to 10 GHz induces up to a 10 dB degradation under both line of sight (LoS) and NLoS conditions [4], [7]. Above 17 GHz, this loss profile steepens further, severely constraining link margins and coverage depth.

To overcome this gap, FR3 networks must rely on compensatory mechanisms such as high-gain directional beamforming—which requires more complex antenna arrays and precise beam control than in FR1—and/or denser network architectures—including microcells, traffic-driven hotspots, and elevation-aware placements. These approaches are essential to maintain target throughput and latency, particularly in urban environments where propagation is highly variable. These dense and directional deployments, however, increase hardware complexity and energy demand, making power efficiency a cross-cutting design priority in future FR3 systems.

2) *Beamforming and Antenna Design Trade-offs*: Bridging the ~10 dB path loss at FR3 necessitates highly directional beams, placing the design burden on practical beamforming realizations and their cost-power trade-offs. Fully digital arrays

deliver the greatest spatial flexibility and multiuser capacity, but their one-transceiver (TRX)-per-element structure drives prohibitive power and data-conversion overheads as array sizes and bandwidths grow. Analog-dominant designs simplify hardware and reduce energy use, yet restrict dynamic beam control and wideband operation [1]. Hybrid beamforming—where antenna elements are combined into fixed radio frequency (RF) subarrays of three to six elements, each driven by a TRX—offers a practical middle ground and is prevalent today. For FR3, its configuration must be re-optimized to handle wideband beam-squint, calibration of large apertures, and scalability in cost and power. The final design balance depends on subarray topology, phase-shifter or true-time-delay networks, and the desired level of digital precoding flexibility, all aiming to enable scalable multi-layer deployments.

3) *Energy Efficiency and Thermal Constraints*: Building on these architectural considerations, energy usage remains one of the most critical bottlenecks for extreme mMIMO in FR3. Current 5G radios already exhibit high power draw, even in idle mode, due to the static energy drain of power amplifiers and always-on TRX chains. A typical configuration with 64 TRX chains and 192 antenna elements consumes over 250 W in idle, with each TRX contributing 2–3 W regardless of traffic load [9].

If 6G systems scale along the same architectural trajectory—toward 128–256 TRX chains and significantly wider bandwidths—, per-radio energy usage at low loads could easily exceed 1 kW [7]. More efficient hardware is essential, yet insufficient on its own. Equally critical is the aggressive use of power-saving mechanisms, including TRX sleep modes and carrier shutdown schemes [10]. Today, these features remain underutilized in live networks, primarily due to operator concerns over coverage degradation and service reliability.

4) *Regulatory Fragmentation and Coexistence Requirements*: The 7–24 GHz spectrum remains fragmented across regions, often shared with radar, satellite, and Earth observation services [5]. For example, 7–8.5 GHz overlaps with radar, 10.7–12.7 GHz with satellite downlinks, and 13.75–14.5 GHz with uplink Earth stations. Coexistence with passive incumbents such as radio astronomy and Earth exploration-satellite service (EESS) requires mitigation strategies like geo-fencing and beam nulling. The pace and scope of international harmonization will directly shape vendor roadmaps and deployment timelines.

III. SYSTEM MODEL FOR DATA-DRIVEN MULTI-LAYER 6G NETWORKS

To explore future deployment strategies and assess their implications on performance and energy usage, we develop a model grounded in a real-world commercial deployment in a dense urban area in China, covering 6.2 km². The model incorporates empirical data from legacy fourth generation (4G) long term evolution (LTE) and operational 5G new radio (NR) networks, including actual BS locations, operating

frequencies, bandwidth allocations, engineering parameters, radio configurations, and traffic load distributions.

Building on this foundation, a synthetic 6G layer is overlaid to simulate prospective deployment scenarios. All simulations are conducted using *Giulia*, which accurately models the behavior of heterogeneous networks using a mix of expert-, 3GPP-, and AI-based models.

A. Multi-Layer Network Deployment

The network comprises three distinct layers:

1) *4G LTE Layer (Empirical)*: The 4G layer is modeled using data extracted directly from the commercial network. It consists of 47 physical sites, each typically configured in a tri-sector layout, amounting to a total of 204 LTE cells. These cells operate across five frequency bands: n3 (1.815 GHz), n34 (2.02 GHz), n39 (1.89 GHz), n40 (2.33 GHz), and n41 (2.62 GHz). This layer exemplifies the heterogeneity of real-world macro-cell deployments in both spectrum use and hardware configuration:

- 184 cells operate with 20 MHz bandwidth, while 20 cells use 10 MHz.
- Transmit power ranges from 40 to 52 dBm, with a median of 45.9 dBm.
- The number of TRXs per cell spans from 2 to 64, with a median of 4. A small subset of LTE cells equipped with 64 TRXs implements mMIMO using planar arrays.

2) *5G NR Layer (Empirical)*: The 5G layer is also modeled based on the empirical deployment data. It consists of 45 NR cells distributed across 15 sites non-co-located with the 4G ones, each operating in band n41 at 2.703 GHz. Unlike the 4G layer, the 5G deployment reflects a more uniform configuration typical of commercial mMIMO rollouts: fixed 100 MHz bandwidth, with 64 TRXs per cell, and a transmit power ranging from 51.3 to 54.7 dBm, with a mean of 53.2 dBm.

3) *6G Layer (Synthetic)*: To explore future deployment strategies, a third layer representing 6G is *synthetically added*. This layer consists of another 45 cells operating at 10 GHz (within the FR3 band), following two distinct placement strategies:

- *Co-located micro cells*: Deployed at the same sites as 5G BSs, using high-power (55 dBm) configurations.
- *Non-co-located cells*: Independently placed at traffic hotspots, using either micro (55 dBm) or pico (52 dBm) radios.

All 6G radios are assumed to operate with 200 or 400 MHz bandwidth and employ 128 or 256 TRXs, enabling advanced spatial multiplexing and highly directional beamforming.

B. User Equipment Distribution (Calibrated from Data)

The spatial distribution of UEs is modeled using a hybrid, data-calibrated approach. Although exact UE coordinates are unavailable, hourly per-cell UE count statistics extracted from live commercial network data provide a robust foundation for realistic traffic modeling.

Focusing on a representative peak-hour snapshot, the number of active UEs per cell is derived directly from these measurements, and uniformly distributed within the corresponding estimated coverage area. The resulting baseline scenario includes 3604 active UEs across the analyzed urban region.

To project the scenario toward future 6G traffic conditions, the baseline is augmented with 15 synthetic traffic hotspots, each randomly located within the most heavily loaded cells. Each hotspot hosts 40 UEs, randomly scattered within a 40 m radius, with a minimum inter-hotspot separation of 80 m to avoid excessive spatial interference coupling.

Finally, each UE is independently classified as indoor or outdoor with an 80% probability of being indoors, reflecting observed user behavior in dense urban environments.

C. Antenna Configurations

BS antenna arrays are inferred from the number of TRXs per cell and calibrated based on known commercial hardware practices:

- 4G: Cells are equipped with vertically oriented, cross-polarized linear arrays. Most radios use compact column configurations (e.g., 2×1, 4×1, or 8×1), while a limited subset of high-capacity sites with 64 TRXs employ 8×4 planar arrays.
- 5G: All cells employ 8×4 cross-polarized planar arrays.
- 6G: Synthetic cells are assumed to use 16×4 or 32×4 cross-polarized planar arrays, depending on whether they have 128 or 256 TRXs. Future cells are modeled with larger planar apertures—either 16 × 16 or 32 × 16 cross-polarized arrays—paired with 128 or 256 TRXs, respectively.

Each antenna element in all arrays is modeled as in [4].

UEs are assumed to be equipped with two cross-polarized antennas, supporting dual-polarization reception for downlink spatial multiplexing.

D. Propagation

The propagation model follows the 3GPP urban macro (UMa) and urban micro (UMi) standard recommendations [4], except for the fast fading component, which is modeled using a Rician distribution, whose K-factor is consistent with such 3GPP guidelines. BSs, whose antenna arrays, are placed at heights greater than 15 m are categorized as UMa, while those below this threshold are treated as UMi.

E. SSB Beam Configuration and Initial Access

Unlike legacy 4G systems that rely on wide-angle, sectorized common reference signals (CRSs), both 5G and 6G define initial access through directional synchronization signal blocks (SSBs) [1]. Here, each SSB is beamformed using a codeword from a 2D-discrete Fourier transform (DFT) codebook and transmitted through a single polarization panel. Crucially, these beams are transmitted sequentially in a time-multiplexed fashion, allowing UEs to detect and evaluate them one at a time. This approach enhances spatial selectivity during initial access, improving coverage and link robustness.

The number of SSB beams per cell increases with each generation to enable finer spatial resolution:

- 5G: All cells use 8 SSB beams.
- 6G: Synthetic cells are assumed to use 16 or 32 SSB beams, depending on whether using 128 or 256 TRXs [2].

During association, each UE measures the reference signal received power (RSRP) of all detected SSB beams and selects the strongest one as its serving beam and corresponding cell. If multiple technologies are available, a priority-based reselection mechanism is applied. Each UE monitors the RSRP of available SSB beams across all technologies, and may reselect to a higher-generation layer if the received signal exceeds a predefined threshold: -110 dBm for 5G and -108 dBm for 6G. This ensures that transitions occur only when higher-generation coverage is strong enough to sustain quality service. We define technology priorities as follows: 0 for 4G, 1 for 5G, and 2 for 6G [2].

F. CSI-RS Beam Codebook and Data Beam Refinement

Following association, beam refinement is assisted by channel state information-reference signals (CSI-RSs), which support spatial multiplexing and precise beam alignment. In line with the Type-I codebook-based channel state information (CSI) feedback framework standardized by 3GPP, each cell transmits a set of precoded CSI-RS beams across both polarization panels. These beams offer finer angular granularity than SSBs, and are constructed using a 2D-DFT codebook that maps antenna geometry into discrete beam directions.

Each UE measures the received power of all available CSI-RSs and reports the index of the preferred beam pair (one per polarization). This feedback enables the serving cell to select the optimal precoding vectors for downlink transmission. Given the two-antenna configuration at the UE side, this mechanism supports dual-layer multiple-input multiple-output (MIMO) and enhances downlink capacity.

The number of CSI-RS beams evaluated in our simulations is as follows:

- 4G: 2, 4, 8, or 64 data beams depending on the number of TRXs per cell.
- 5G: 64 CSI-RS beams per cell, supporting adaptive spatial multiplexing.
- 6G: 128 or 256 CSI-RS beams per cell, depending on the number of TRXs, 128 or 256, enabling high-resolution multi-user MIMO [2].

G. Traffic-Aware Scheduling Based on CSI-RS Beam Selection

The scheduler operates on a data-driven traffic model, where physical resource block (PRB) demands are inferred from real-world network measurements. Specifically, we leverage hourly deployment statistics—such as the average number of PRBs utilized per cell and the number of active UEs—to estimate per-UE demand. By dividing total PRB usage by the number of active UEs, we obtain a reliable estimate of average per-UE PRB requirement, which directly guides the resource allocation process.

Each UE is equipped with two cross-polarized antennas and configured to receive two spatial streams, enabling dual-layer MIMO transmission. To support this, the scheduler assigns each UE a pair of CSI-RS beams—one per polarization—selected based on the highest measured RSRP, following the refinement procedure described earlier.

PRBs are allocated independently on a per-beam basis. Initially, all PRBs within each beam are unassigned. UEs are then randomly allocated PRBs within their selected beam, in proportion to their estimated demand, until either the demand is fulfilled or the PRB pool of the beam is exhausted. This random allocation strategy is justified by the inherent channel hardening effect of mMIMO, which significantly reduces per-PRB channel variability [1].

H. Performance Metrics

To drive the simulations and evaluate the effectiveness of each deployment strategy, we assess the following three key performance metrics:

1) *SINR and Effective SINR*: The instantaneous signal-to-interference-plus-noise ratio (SINR) is computed per PRB and per MIMO layer, accounting for transmit power, beamforming gain, path loss, shadowing, fast fading, inter-cell interference, and thermal noise, in accordance with the adopted 3GPP UMa/UMi channel model [4].

Under the embraced dual-layer MIMO scheduling configuration—where each UE is assigned two spatial streams—the resulting per-PRB and per-layer SINRs are aggregated into a single effective SINR per layer (codeword) using a mutual information-based mapping [11]. This effective SINRs determines the modulation and coding schemes (MCSs) that can be reliably supported under prevailing channel and interference conditions.

2) *Achievable UE Rate*: The achievable downlink rate for each UE is determined by three factors: the effective SINR, the number of PRBs allocated via the data-driven scheduling process, and the spatial multiplexing gain provided by dual-layer MIMO. The effective SINR governs the MCS applied per MIMO layer, thereby defining the spectral efficiency achieved on each stream. By combining the spectral efficiency with the number of active layers and allocated PRBs, we obtain a realistic estimate of per-UE throughput, serving as a key indicator of user experience across deployment scenarios.

3) *Power Usage*: Since different radio technologies exhibit distinct power consumption characteristics, we adopt a *data-driven, machine learning-based* model to estimate the energy usage of each radio unit across the evaluated deployments. The model is trained on empirical measurements from commercial multi-technology, multi-band radios and employs an artificial neural network (ANN) to capture the relationship between power draw, hardware configuration, and traffic load [12].

For 4G and 5G radios, all model parameters are directly derived from real-world deployment data. In contrast, for 6G radios, energy usage is estimated by scaling the 5G model according to forward-looking yet conservative assumptions on

component-level efficiency improvements, yielding a lower-bound estimate of future 6G power consumption.

The model also reflects the architectural differences among generations. The 4G radios, typically co-located across multiple frequency bands, may employ multicarrier power amplifiers (MCpas) to amplify spectrally adjacent carriers using shared amplifier chains, while widely separated carriers operate on independent power stages. The non-co-located 5G radios, by contrast, use active antenna units (AAUs) with dedicated amplifier per TRX, enabling full digital beamforming at the cost of higher per-chain baseline consumption. In our 6G deployments—whether co-located with 5G or not—each layer is realized through an independent radio unit, given the large frequency separation between 5G and 6G carriers.

The total power consumption of each radio is decomposed into five key components:

- *Baseline power consumption*: Energy used by always-on circuitry, such as monitoring, synchronization, and control modules.
- *Baseband processing power*: Computational load required for digital signal processing in AAUs.
- *Transceiver power*: Energy drawn by the TRXs, encompassing digital-to-analog and upconversion.
- *Power amplifier overhead*: Static bias power required to maintain amplifier readiness. In 4G, this may correspond to a shared MCPA per band, whereas in 5G and 6G, each TRX integrates its own wideband amplifier.
- *Radiated output power (P_{out})*: Power needed to generate the transmit signal across the cells served by the radio. This component depends on amplifier and antenna efficiency, and scales with the allocated transmission power.

IV. PERFORMANCE ANALYSIS

Leveraging our real-world deployment and traffic data from a commercial 4G/5G network in China, we conduct a performance analysis of heterogeneous 4G/5G/6G networks using Giulia.

A. Deployment Strategies Evaluated

The five deployment configurations analyzed are:

- 4G UMa: Baseline deployment consisting solely of legacy 4G LTE macrocells.
- 4G + 5G UMa: Empirical dual-layer network with non-co-located 4G LTE and 5G NR macrocells.
- 4G + [5G + 6G UMa] (co-located): Addition of 6G macro cells at existing 5G site locations to enhance bandwidth and spatial multiplexing.
- 4G + 5G + 6G UMi (non-co-located): Independent deployment of 6G microcells targeted at traffic hotspots for localized capacity boosts.
- 4G + 5G + 6G UPi (non-co-located): Energy-efficient configuration deploying low-power 6G urban pico (UPi) cells at hotspot locations.

Fig. 1 provides a visual representation of the 4G + 5G + 6G UPi (non-co-located) deployment, highlighting the spatial distribution of the 4G, 5G, and 6G sites, and

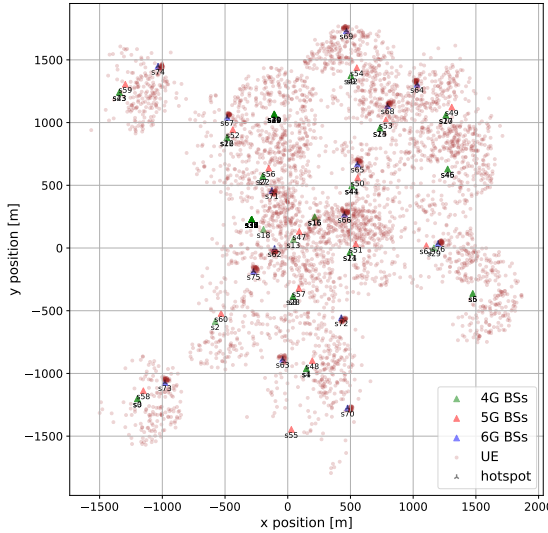


Fig. 1: Spatial network layout, along with UE distribution.

the corresponding UE deployment, including hotspot locations. Tab. I provides a summary of cells characteristics per technology.

B. UE Throughput

Fig. 2 illustrates the distribution of downlink UE rates for all scenarios. Key statistics—including mean, 5%-tile, 50%-tile, and 95%-tile values—are summarized in Table II.

The baseline 4G UMa delivers a mean UE throughput of 14.33 Mbps and a 5%-tile of 0.40 Mbps, reflecting 20 MHz spectrum and simple antenna arrays. Adding a 5G layer (4G UMa + 5G UMa) lifts the mean by +77% and the 5%-tile by 2.4×, due to 100 MHz bandwidth and 64-TRX mMIMO.

Introducing a 6G layer operating in FR3 yields substantial further gains. With 200 MHz bandwidth and 128 beams, co-located 6G macros (4G UMa + [5G UMa + 6G UMa]) already triple the mean and raise the 5%-tile by 70% relative to the 4G UMa + 5G UMa baseline. Yet the most significant improvements occur when 6G nodes are deployed closer to UEs. Non-co-located 6G micro (6G UMi) and pico/hotspot

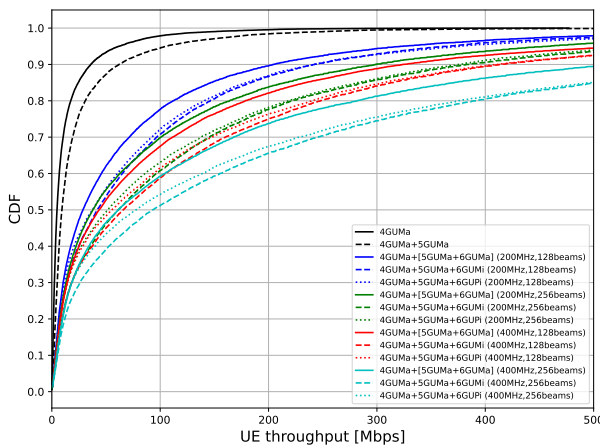


Fig. 2: Downlink UE throughput across deployment scenarios.

(6G UPi) deployments reduce path loss and improve link geometry, pushing the 5%-tile throughput up by 1.81–2.1× and the mean by 3.7–3.8× compared with 4G UMa + 5G UMa. The 6G UMi provides better performance than 6G UPi due to the larger transmit power. This confirms that proximity and spatial densification, rather than merely co-locating new layers, are key to unlocking FR3 capacity.

Considering a 200 MHz bandwidth, increasing the beam count from 128 to 256 in the non-co-located 6G micro-cell (6G UMi) deployment improves the 5%-tile by approximately 18% and the mean by about 48% (corresponding to 2.4× and 5.6× w.r.t. 4G UMa + 5G UMa) thanks to finer spatial reuse and narrower beam footprints. However, expanding bandwidth to 400 MHz, while keeping 128 beams, provides comparable or slightly higher aggregate gains: the 5%-tile stays the same w.r.t. 200 MHz bandwidth and 256 beams, the mean improves another 13%, while the 95%-tile rises by 11%. These results highlight a practical trade-off between spatial multiplexing and bandwidth expansion that operators must carefully evaluate.

Among all cases, the 400 MHz, 256-beam, non-co-located 6G UMi is best overall, delivering ≈9.9× mean, ≈2.8× 5%-tile, ≈10× 50%-tile, and ≈9.7× 95%-tile gains relative to 4G UMa + 5G UMa. These improvements highlight that closer, data-driven 6G deployments in FR3 bands dramatically enhance both average capacity and user-experience uniformity, demonstrating that proximity-aware densification—not mere co-location—is the decisive factor in realizing FR3's full potential.

C. Network Power Consumption

Figure 3 illustrates the average total power consumption of the network for each deployment strategy. These results highlight the energy trade-offs associated with densification and new-layer integration.

The 4G UMa baseline consumes 112 kW, i.e., –30% relative to the 4G UMa + 5G UMa benchmark at 160 kW, reflecting the additional bandwidth and activation of 64-TRX mMIMO. Introducing 6G layers in FR3 increases absolute network power due to wider bandwidths and a larger number of

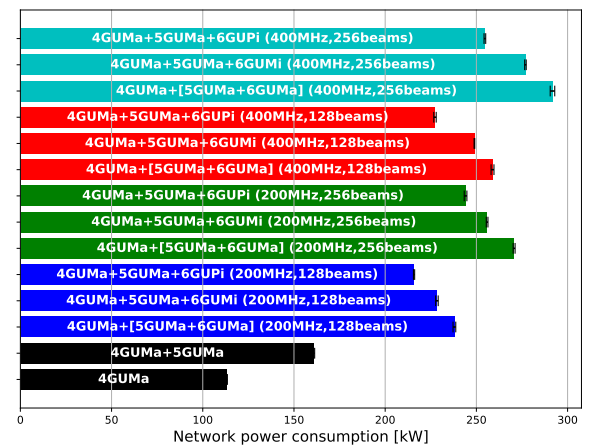


Fig. 3: Average network power consumption across scenarios.

TABLE I: Data-derived characteristics of 4G and 5G, and those assumed for 6G radios.

Radio	Carrier freq. [GHz]	Bandwidth [MHz]	PRBs	# cells	TRXs (M^{TRX})	TX power [dBm]	Antenna elements	SSB beams	CSI-RS beams
4G UMa (LTE)	1.815–2.664	10–20 (mean = 19.1)	100	204	2–64 (50 %-tile = 4)	40–52 (50 %-tile = 45.9)	8 (linear)–64 (8×4 dual-pol)	1	2–8
5G UMa (NR)	2.703	100	273	45	64	51.3–54.7 (mean 53.2)	64 (8×4 dual-pol)	8	64
6G UMa/UMi	10	200/400	273	45	128/256	55 (58)	128 (16×4 dual-pol)*	16/32 (assumed)	128/256 (assumed)
6G UPi	10	200/400	273	45	128/256	52 (55)	128 (16×4 dual-pol)*	16/32 (assumed)	128/256 (assumed)

* Double in case of 256 TRX with (16×4 dual-pol) and (32×4 dual-pol).

TABLE II: Estimated downlink UE throughput statistics derived from the CDF curves (mean, 5%, 50%, and 95% percentiles).

Configuration	Scenario	Mean [Mbps]	5%-tile [Mbps]	50%-tile [Mbps]	95%-tile [Mbps]	Power [kW]
As per data	4G UMa	14.33 (-43%)	0.40 (-58%)	4.79 (-48%)	61.79 (-42%)	112 (-30%)
As per data	4G UMa + 5G UMa	25.34 (1×)	0.95 (1×)	9.27 (1×)	105.55 (1×)	160 (1×)
200MHz/128TRX	4G UMa + [5G UMa + 6G UMa]	78.93 (×3.1)	1.62 (+70%)	28.70 (×3.1)	324.31 (×3.1)	238 (+49%)
	4G UMa + 5G UMa + 6G UMi	95.99 (×3.8)	1.96 (×2.1)	41.82 (×4.5)	365.78 (×3.5)	228 (+43%)
	4G UMa + 5G UMa + 6G UPi	94.18 (×3.7)	1.73 (+81%)	37.24 (×4.0)	376.62 (×3.6)	215 (+34%)
200MHz/256TRX	4G UMa + [5G UMa + 6G UMa]	109.38 (×4.3)	1.76 (+85%)	37.82 (×4.1)	457.53 (×4.3)	270 (+69%)
	4G UMa + 5G UMa + 6G UMi	142.44 (×5.6)	2.32 (×2.4)	61.20 (×6.6)	573.16 (×5.4)	255 (+59%)
	4G UMa + 5G UMa + 6G UPi	135.43 (×5.3)	1.94 (×2.0)	51.74 (×5.6)	544.68 (×5.2)	245 (+53%)
400MHz/128TRX	4G UMa + [5G UMa + 6G UMa]	128.86 (×5.1)	1.89 (+98%)	43.67 (×4.7)	531.42 (×5.0)	260 (+63%)
	4G UMa + 5G UMa + 6G UMi	161.79 (×6.4)	2.33 (×2.4)	65.83 (×7.1)	638.68 (×6.0)	250 (+56%)
	4G UMa + 5G UMa + 6G UPi	156.32 (×6.2)	2.05 (×2.1)	55.35 (×6.0)	642.97 (×6.1)	228 (+43%)
400MHz/256TRX	4G UMa + [5G UMa + 6G UMa]	192.59 (×7.6)	2.42 (×2.5)	61.27 (×6.6)	829.62 (×7.9)	292 (+83%)
	4G UMa + 5G UMa + 6G UMi	249.89 (×9.9)	2.68 (×2.8)	92.88 (×10.0)	1027.62 (×9.7)	275 (+72%)
	4G UMa + 5G UMa + 6G UPi	240.34 (×9.5)	2.35 (×2.5)	77.84 (×8.4)	1014.80 (×9.6)	255 (+59%)

active transceiver chains. In our model, each TRX contributes approximately 1.5–3 W, leading to near-linear power scaling when the TRX count increases (e.g., 128→256).

At 200 MHz/128TRX, the co-located 4G UMa + [5G UMa + 6G UMa] configuration reaches 238 kW (+49 % vs. 4G UMa + 5G UMa), whereas closer-to-the-UE non-co-located 6G UMi and 6G UPi deployments require only 228 kW (+43 %) and 215 kW (+34 %), respectively, while delivering substantially higher throughput, as shown earlier. This indicates that improved link geometry reduces the required transmit power, limiting the growth of network power despite densification.

More generally, the results highlight a clear throughput–energy trade-off: capacity gains come at the cost of higher power, but the increase is sub-linear relative to throughput. Notably, the 400 MHz/128TRX operating point is slightly less power-hungry than 200 MHz/256TRX at comparable throughput, because doubling the number of transceiver chains introduces a hardware power penalty that can outweigh the additional bandwidth-dependent processing (and the associated transmit-power setting in the 400 MHz mode).

Overall, while FR3 evolution inevitably raises absolute network power consumption, proximity-aware densification and careful bandwidth/TRX dimensioning allow operators to achieve large throughput gains with a moderate and controlled energy increase, yielding a more favorable power–throughput operating regime than co-located macro-layer upgrades.

V. CONCLUSION

This work evaluated the performance and energy implications of multi-layer 6G evolution using a data-driven model grounded in a live urban 4G/5G deployment and an FR3-based 6G extension. The results show that FR3 can unlock order-of-magnitude capacity gains, but only when new layers are deployed based on traffic and spatial data rather than convenience-driven co-location. In particular, a non-co-located 6G UPi / HS hotspot deployment achieves approximately 9.5×

higher mean UE throughput while increasing total network power by only 59 % relative to the 4G UMa + 5G UMa baseline. This demonstrates that substantial capacity improvements can be obtained with a controlled energy cost when 6G nodes are placed close to demand hotspots. Overall, the findings indicate that realizing the full potential of FR3 is not merely a question of spectrum availability or radio hardware, but a deployment optimization problem. Data-driven, proximity-aware densification is essential to maximize throughput gains per unit of energy and to enable practical, scalable, and sustainable 6G networks.

REFERENCES

- [1] E. Dahlman *et al.*, *5G/5G-Advanced: The New Generation Wireless Access Technology*. Academic Press, 2023.
- [2] D. López-Pérez *et al.*, “Capacity and Power Consumption of Multi-Layer 6G Networks Using the Upper Mid-Band,” in *Proc. IEEE Int. Conf. on Comm. (ICC)*, 2025, pp. 1–6.
- [3] E. Björnson *et al.*, “Enabling 6G Performance in the Upper Mid-Band by Transitioning From Massive to Gigantic MIMO,” *IEEE Open J. ComSoc*, pp. 1–14, 2025.
- [4] 3GPP Technical Report 38.901, “Study on channel model for frequencies from 0.5 to 100 GHz (Release 18),” Apr. 2024.
- [5] 3GPP Technical Report 38.820, “7–24 GHz frequency range (Release 16),” Jul. 2021.
- [6] Nokia, “Coverage evaluation of 7–15 GHz bands from existing sites,” 2024.
- [7] Huawei, “Centimeter-wave-MIMO: A key enabler for 6G,” 2024.
- [8] S. Kang *et al.*, “Cellular wireless networks in the upper mid-band,” *IEEE Open J. ComSoc*, vol. 5, pp. 2058–2075, 2024.
- [9] Nokia, “Extreme massive MIMO for macro cell capacity boost in 5G-Advanced and 6G,” 2023.
- [10] D. López-Pérez *et al.*, “A survey on 5G radio access network energy efficiency: Massive MIMO, lean carrier design, sleep modes, and machine learning,” *IEEE Commun. Surveys Tuts.*, vol. 24, no. 1, pp. 653–697, 2022.
- [11] K. Brueninghaus *et al.*, “Link performance models for system level simulations of broadband radio access systems,” in *Proc. IEEE Int. Symp. on Personal, Indoor and Mob. Radio Commun. (PIMRC)*, 2005, pp. 2306–2311.
- [12] N. Piovesan *et al.*, “Machine learning and analytical power consumption models for 5G base stations,” *IEEE Commun. Mag.*, vol. 60, no. 10, October 2022.